Correspondence

The slow-growing tooth of the Amery Ice Shelf from 2004 to 2012

The Loose Tooth rift system is an active rift system located at the front of the Amery Ice Shelf, Antarctica, which is expected to calve and produce a large iceberg in the near future. A time series of Envisat advanced synthetic aperture radar (ASAR) images from February 2004 to February 2012 has been used here to observe the system. The results show that both the west (T1) and east (T2) rifts propagated rapidly over 9 years at average rates of 4.49 and 2.53 m d^{-1}, respectively. The rift system will not break during 2012–15 as previously projected, unless unforeseen events occur. Additionally, it was found that the heading direction of T1 turned dramatically in 2009–10. However, most surprising is that the propagation rates of both rifts have shown a decreasing trend since 2005, which might be due to increasing thickness of melange ice filling in the rifts. Other environmental factors (e.g. wind forcing and air temperature) may influence the rift motion by changing the melange ice thickness and other properties.

INTRODUCTION

Antarctic ice shelves are prominent, constituent parts of ice sheets due to their ice–ocean–atmosphere interface and their vulnerability to regional and global changes in atmospheric and oceanic temperatures (Mercer, 1978; Vaughan and Doake, 1996; Shepherd and others, 2004). The majority of mass loss from the Antarctic ice sheet is from ice shelves via either iceberg calving (the production of icebergs that break off from the ice shelf) or basal melting (the melting of ice at the bottom of the ice shelf due to warmer ocean temperatures or increased pressure) (Jacobs and others, 1992; Williams and others, 2002). Iceberg calving events are sporadic, but occur in a natural cycle of advance and retreat of the ice-shelf front over periods typically lasting several decades (Budd, 1966; Scambos and others, 2003).

The retreat and disintegration of several ice shelves during the past few decades (Rott and others, 2002; De Angelis and Skvarca, 2003; Braun and others, 2009) has raised significant concerns that these occurrences could become more frequent in a warming climate (Janssen, 2009). As a result, large amounts of mass could be removed nearly instantaneously with calving events (Bassis and others, 2008). The collapse of the Larsen B ice shelf (Rignot and others, 2004; Scambos and others, 2004) has proven that ice shelves are dynamically coupled with the flow of inland ice and can modulate ice flow far upstream of the grounding line. This phenomenon affects the discharge of grounded ice and has a direct influence on sea-level rise (Bassis and others, 2008). To fully understand the processes behind changes in ice-shelf rifting systems and the interactions between the atmosphere, ocean and ice, it is necessary to monitor such systems over an extended period of time.

The Amery Ice Shelf is the largest ice shelf in East Antarctica (Fig. 1a). It drains continental ice from an area of $>10^6$ km^2 (Allison, 1991) through a section of coastline that represents ~2% of the total continental circumference (Budd and others, 1967). The last major calving event occurred in late 1963 or early 1964, when a ~10 000 km^2 iceberg detached itself from the Amery Ice Shelf, removing nearly one-seventh of the shelf's total surface area (Budd, 1966; Fricker and others, 2002a,b). A precursor to calving is the initiation and subsequent propagation of rifts, which penetrate the entire ice shelf (Fricker and others, 2005). Rifts propagate and widen until they eventually become detachment boundaries for tabular icebergs. The Loose Tooth (LT) rift system (Fig. 1c) is an active rift system located at the front of the Amery Ice Shelf, which is likely to calve and produce a large iceberg in the near future. Additionally, an analysis of historical data indicates that a similar Loose Tooth-sized calving event preceded the last major calving event of 1963–64 (Fricker and others, 2002a).

The system consists of two longitudinal-to-flow rifts ~30 km apart that were shaped over the 1980s (denoted L1 and L2), and two transverse-to-flow rifts (denoted T1 and T2) that were initiated at the tip of L1 in 1995, when L1 was 23 km long (Fricker and others, 2002a, 2005; Bassis and others, 2005). Meanwhile, the longitudinal-to-flow strain rates began to exceed transverse-to-flow strain rates (Young and Hyland, 2002), and L2 stopped propagating (Fricker and others, 2005). There are two other longitudinal-to-flow rifts west of the LT rift system (denoted L3 and L4). The T2 tip propagated at ~4 m d^{-1} from late 1999 to early 2004, exhibiting a seasonal dependence with significantly higher rates during the austral summer period (Fricker and others, 2005); however, a slowing trend of rift T2 has recently been reported (Bassis and others, 2007).

DATA AND METHOD

To quantify the rift changes, we measured the rift length over 9 years (February 2004 to February 2012) using Envisat ASAR data. Antarctic sea ice peaks in September (at the end of the Southern Hemisphere winter) and retreats to a minimum in February–March. From February 2004 to February 2012 we gathered data from Envisat ASAR, which operates in the C-band (5.6 cm wavelength), on the LT rift system in wide swath mode.

All Envisat ASAR data were processed with precise orbits and geometric corrections. We obtained images at a 75 m resolution with registration accuracy within one pixel. The histogram of each image was linearly stretched to enhance the rifts and then filtered according to an efficient image-denoising scheme using principal component analysis with local pixel grouping (Zhang and others, 2010). We then extracted the rift edges semi-automatically by combining an artificial drawing method with an improved watershed algorithm (Wang and others, 2010). The rift lengths were estimated diagonally along the upstream rift wall according to the extracted edges from point 'V' in the triple junction (Fig. 1c) to the rift tips.

RESULTS AND DISCUSSION

There has been an increase in the lengths and widths of both rift T1 and T2 over the past 9 years (Fig. 2). From 2004 to 2012, T1 lengthened from 5.3 to 18.3 km and T2 propagated from 17.0 to 24.3 km (Fig. 3a). T1 is propagating at ~4.49 m d^{-1}, while T2 is growing at ~2.53 m d^{-1}. Assuming that rift T2 will propagate at an average rate of ~2.53 m d^{-1}

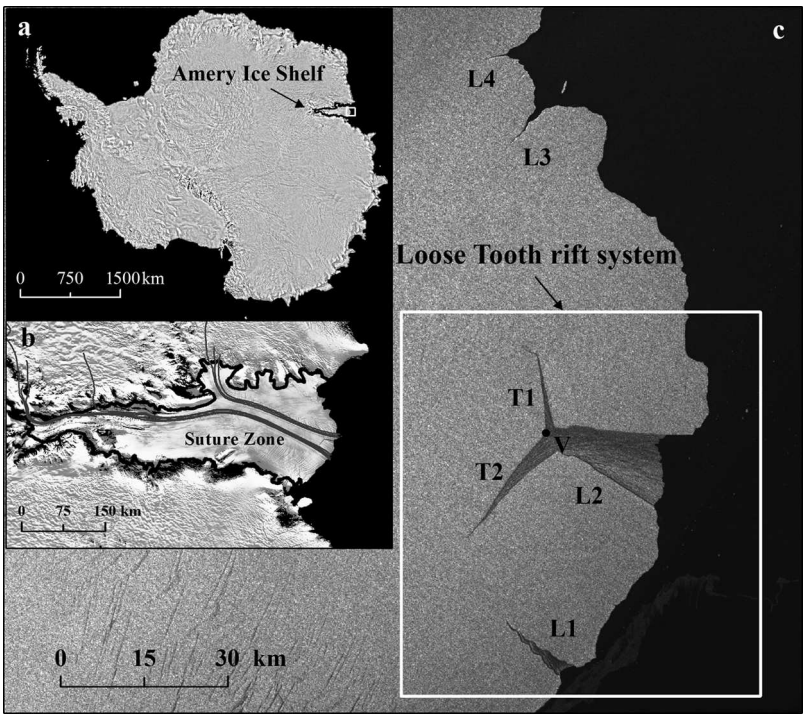

Fig. 1. The Loose Tooth rift system. (a) MODIS Mosaic of Antarctica (MOA), 29 February 2004 (Haran and others, 2005), showing the location of the Amery Ice Shelf in East Antarctica. (b) Map showing the formation of suture zone where two ice streams merged (gray curve). (c) Envisat ASAR image acquired on 11 February 2011 showing an enlarged view of the Loose Tooth rift system.

from 2013 to 2015, an iceberg between T2 and L1 will not calve during 2012–15, as projected previously by Fricker and others (2005). The exception is, of course, the occurrence of unforeseen events, including significant seismic activities or tsunami, as was the case with the iceberg break-off from the Sulzberger and Ross Ice Shelves (MacAyeal and others, 2009; Brunt and others, 2011). Rift T1 started to grow southward in February 2009 and then westward in February 2010 (Fig. 2).

Combining the measurement results from Fricker and others (2005) with the data in Figure 3a, Figure 3b indicates that rift T1 has had a higher propagation rate than rift T2 since 2004. However, the propagation rates of both rifts show a similar trend over the past 9 years (Fig. 3b), increasing from 2004 to 2005, 2008 to 2009, and 2010 to 2011, and decreasing from 2006 to 2007, 2009 to 2010, and 2011 to 2012. Furthermore, propagation rates of rift T1 have decreased more significantly than those of rift T2 since 2009, when rift T1 started to grow southward and then westward, almost parallel to the ice flow. We surmise that the changing distributions of the strain field in the rift tip might stop the rift forward. On the whole, both rifts show a retarding trend since 2005; Bassis and others (2007) also

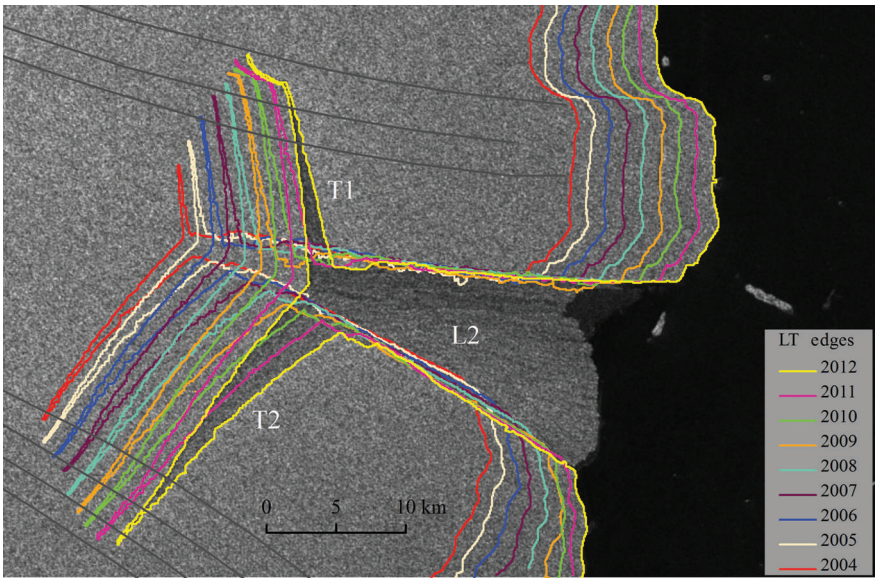

Fig. 2. Loose Tooth edges extracted from Envisat ASAR (2004–12) with the background image of Envisat ASAR on 17 February 2012. The gray curve is the suture zone formed where two ice streams merged.

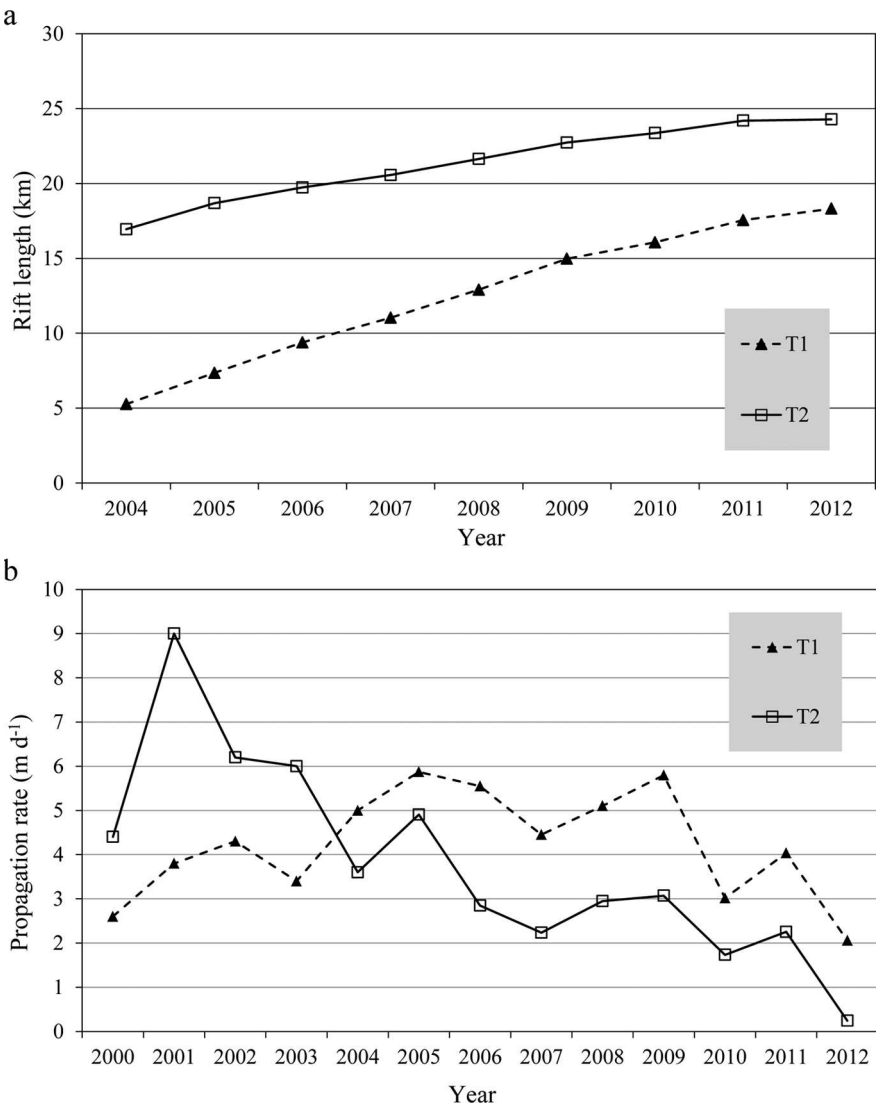

Fig. 3. Rift length and propagation rate. (a) Measured rift lengths derived from Envisat ASAR from February 2004 to February 2012. The slopes of the solid line and dotted line show that rift T1 has had a higher propagation rate than rift T2 since 2004. (b) Propagation rates for every 2 years from 2000 to 2012. The data from 2000 to 2012 are from Fricker and others (2005). The solid line shows the slowing of rift T2. The solid and dotted lines show a similar trend for both rifts since 2004.

found an overall decrease in propagation rates for T2 between 2000 and 2006.

Evidence has been presented that rift propagation occurs in episodic bursts, primarily driven by the internal stress in the ice shelf caused by the gravitational spreading of the ice. This evidence opposes the idea that short-term environmental forces (e.g. winds or ocean tides) can initiate propagation (Bassis and others, 2005, 2008; Joughin and MacAyeal, 2005; Janssen, 2009). Internal stress is also a dominant force in rift widening (Joughin and MacAyeal, 2005). Rift widths increase steadily at a rate similar to that of ice-shelf spreading, whereas rift lengths grow episodically by the coalescence of several discrete rift-tip propagation bursts, occurring as a series of micro- and mesoscale cracks ahead of the rift tips (Schulson, 2001; Bassis and others, 2005, 2007; Joughin and MacAyeal, 2005). According to Weertman (1957), the stress, τ_i, within the ice shelf is related to ice thickness and the densities of ice and water:

$$\tau_i = \rho_i g H_i \left(1 - \frac{\rho_i}{\rho_w}\right), \quad (1)$$

where ρ_i is the density of the ice, ρ_w is the density of the sea water and H_i is the ice thickness. The Amery Ice Shelf elevation change rate during 2003–08 is $-0.06 \pm 0.008\ m\ a^{-1}$ (Pritchard and others, 2012), and the thickness change rate during 1994–2008 is $0.92\ m\ a^{-1}$ (Shepherd and others, 2010). Following Eqn (1), large-scale stress is relatively constant during 1994–2008, as the ice thickness change is relatively small in proportion to the ice thickness (~270 m near the LT rift system (Craven and others, 2009)).

However, melange, which fills the rifts and is composed of sea ice, accumulated and wind-blown snow, ice fragments broken off the ice shelf, and marine ice may modulate the stress field (Rignot and MacAyeal, 1998; Khazendar and Jenkins, 2003; Fricker and others, 2005). It has been suggested that melange may impede rift propagation and iceberg calving (Hulbe and others, 1998; Rignot and MacAyeal, 1998) by viscous coupling, and thick melange may likewise slow propagation (Larour and others, 2004; Fricker and others, 2005). With its seasonally variable characteristics and side-walls that are thinner than the rift, melange may melt more easily than the surrounding ice shelf due to ocean warming (Rignot and MacAyeal, 1998; Larour and others, 2004; Fricker and others, 2005). The

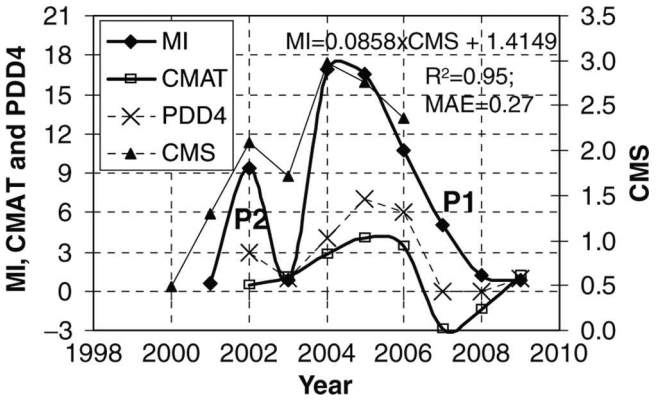

Fig. 4. Interannual variations of the melting index (MI), cumulative melting surface (CMS), cumulative monthly mean air temperature (CMAT) and the number of positive degree-days with temperatures greater than 4°C (PDD4) for the month of January from 1998 to 2010 over the AIS (Oza and others, 2011).

composition as well as the accumulation and attrition process of melange ice may be a key factor in rift propagation.

Oza and others (2011) studied the interannual variations in surface melting over the Amery Ice Shelf from 2000 to 2009, showing a decreasing trend in surface melting since 2005 (melting index (MI) and cumulative melting surface (CMS) in Fig. 4). Craven and others (2009) estimated a snow accumulation rate of $0.71 \pm 0.08\,\mathrm{m\,a^{-1}}$ near the LT. In addition, the basal melting rate of the Amery Ice Shelf dramatically decreases from the southern grounding zone to the downstream ice shelf; the basal melting rate at the front is $-9.5 \pm 5.6\,\mathrm{Gt\,a^{-1}}$, with a net basal refreezing rate of $0.2 \pm 0.1\,\mathrm{m\,a^{-1}}$ (Yu and others, 2010). Wen and others (2010) also calculated the spatial distribution of the basal melting/freezing rates ($\mathrm{m\,a^{-1}}$) beneath the Amery Ice Shelf, and found that the tips of both rifts are located within the freeze-on area. There remains a significant amount of marine ice formed in the calving front through the refreezing process, originally found by Fricker and others (2001), which could bind the ice blocks together, give the melange more mechanical strength, and slow rift propagation (Bassis and others, 2007). The average accretion rate of marine ice near the calving front is $1.1 \pm 0.2\,\mathrm{m\,a^{-1}}$. We speculate that the melange thickness in LT might be increasing with the decrease of surface and basal melting, the increase of surface accumulation and basal refreezing. This would slow rift propagation.

As an external forcing for rifts, wind forcing could influence the amount of wind-transported snow, as well as the surface and basal melting rates (Leonard and others, 2008; Pritchard and others, 2012). Such influences could then affect the rift motion over a long-term scale. Moreover, the changing propagation rates of both rifts (Fig. 3b) share a similar trend with air temperature (CMAT in Fig. 4) and the number of positive degree-days with temperatures greater than 4°C (PDD4 in Fig. 4) for January 2004–09 (Oza and others, 2011), indicating that air temperature is an important environmental force. Both wind forcing and air temperatures may influence rift propagation by affecting the melange ice thickness and other properties, which further demonstrates that melange ice is a key influencer in rift motion. Additionally, tips of both rifts encountered suture zones (Figs 1b and 2), which could reduce stress concentrations ahead of the rift tips (Bassis and others, 2007), potentially hindering them.

CONCLUSION

Time-series observations of the LT rift system from 2004 demonstrate the obvious propagation and widening of two rifts, primarily driven by internal stress. With an average propagating speed of $4.49\,\mathrm{m\,d^{-1}}$ for T1 and $2.53\,\mathrm{m\,d^{-1}}$ for T2 and barring the occurrence of any unforeseen events, the rift will not break during 2012–15 as previously projected by Fricker and others (2005). Rift T1 has changed its propagation direction since 2009. Moreover, rift T1 has had a higher propagation rate than rift T2 since 2004; however, the propagation rates of both rifts have shown a similar downturn since 2005. Thickening melange ice in the rifts or an encounter with the suture zone could potentially affect propagation rates. Wind-forcing and air-temperature changes may lead to changes in the melange ice, consequently impacting rift development. As to the undetermined factors, additional field studies and autonomous observations are necessary to further enhance our understanding of rift propagation mechanisms and to predict calving times.

ACKNOWLEDGEMENTS

This work was supported by the Chinese Arctic and Antarctic Administration, National Basic Research Program of China (grant No. 2012CB957704), National Natural Science Foundation of China (grant Nos. 41176163 and 41106157), National High-tech R&D Program of China (grant Nos. 2008AA121702 and 2008AA09Z117) and China Postdoctoral Science Foundation (No. 201104063). We thank L. Wang for providing the filtering processing program and edge extraction program, and K.C. Wang and L.N. Wang for critical discussions and valuable opinions. We thank the anonymous reviewers for valuable comments and suggestions.

State Key Laboratory of Remote Sensing Science,
Beijing Normal University and
Institute of Remote Sensing and Digital Earth,
Chinese Academy of Sciences,
Beijing, China
E-mail: chenzhao1989ice@gmail.com

Chen ZHAO*
Xiao CHENG*
Yan LIU*
Fengming HUI*
Jing KANG*
Xianwei WANG*
Fang WANG*
Cheng CHENG*

**College of Global Change and Earth System Science,*
Beijing Normal University,
Beijing, China

REFERENCES

Allison I (1991) The Lambert Glacier/Amery Ice Shelf study: 1988–1991. *Aurora*, **10**(4), 22–25

Bassis JN, Coleman R, Fricker HA and Minster JB (2005) Episodic propagation of a rift on the Amery Ice Shelf, East Antarctica. *Geophys. Res. Lett.*, **32**(6), L06502 (doi: 10.1029/2004GL022048)

Bassis JN and 7 others (2007) Seismicity and deformation associated with ice-shelf rift propagation. *J. Glaciol.*, **53**(183), 523–536 (doi: 10.3189/002214307784409207)

Bassis JN, Fricker HA, Coleman R and Minster J-B (2008) An investigation into the forces that drive ice-shelf rift propagation

on the Amery Ice Shelf, East Antarctica. *J. Glaciol.*, **54**(184), 17–27 (doi: 10.3189/002214308784409116)

Braun M, Humbert A and Moll A (2009) Changes of Wilkins Ice Shelf over the past 15 years and inferences on its stability. *Cryosphere*, **3**(1), 41–56

Brunt KM, Okal EA and MacAyeal DR (2011) Antarctic ice-shelf calving triggered by the Honshu (Japan) earthquake and tsunami, March 2011. *J. Glaciol.*, **57**(205), 785–788 (doi: 10.3189/002214311798043681)

Budd W (1966) The dynamics of the Amery Ice Shelf. *J. Glaciol.*, **6**(45), 335–358

Budd W, Smith IL and Wishart E (1967) The Amery Ice Shelf. In Oura H ed. *Physics of snow and ice*. (ANARE Reprint 1, Part 1) Institute of Low Temperature Science, Hokkaido University, Sapporo, 447–467 **[[AUTHOR: please check series number]]**

Craven M, Allison I, Fricker HA and Warner R (2009) Properties of a marine ice layer under the Amery Ice Shelf, East Antarctica. *J. Glaciol.*, **55**(192), 717–728 (doi: 10.3189/002214309789470941)

De Angelis H and Skvarca P (2003) Glacier surge after ice shelf collapse. *Science*, **299**(5612), 1560–1562 (doi: 10.1126/science.1077987)

Fricker HA, Popov S, Allison I and Young N (2001) Distribution of marine ice beneath the Amery Ice Shelf. *Geophys. Res. Lett.*, **28**(11), 2241–2244 (doi: 10.1029/2000GL012461)

Fricker HA, Young NW, Allison I and Coleman R (2002) Iceberg calving from the Amery Ice Shelf, East Antarctica. *Ann. Glaciol.*, **34**, 241–246 (doi: 10.3189/172756402781817581)

Fricker HA and 9 others (2002) Redefinition of the Amery Ice Shelf, East Antarctica, grounding zone. *J. Geophys. Res.*, **107**(B5), 2092 (doi: 10.1029/2001JB000383)

Fricker HA, Young NW, Coleman R, Bassis JN and Minster JB (2005) Multi-year monitoring of rift propagation on the Amery Ice Shelf, East Antarctica. *Geophys. Res. Lett.*, **32**(2), L02502 (doi: 10.1029/2004GL021036)

Haran T, Bohlander J, Scambos T, Fahnestock M and compilers (2005) *MODIS mosaic of Antarctica (MOA) image map*. National Snow and Ice Center, Boulder, CO. Digital media: http://nsidc.org/data/nsidc-0280.html

Hulbe CL, Rignot E and MacAyeal DR (1998) Comparison of ice-shelf creep flow simulations with ice-front motion of Filchner–Ronne Ice Shelf, Antarctica, detected by SAR interferometry. *Ann. Glaciol.*, **27**, 182–186

Jacobs SS, Hellmer HH, Doake CSM, Jenkins A and Frolich RM (1992) Melting of ice shelves and the mass balance of Antarctica. *J. Glaciol.*, **38**(130), 375–387

Janssen V (2009) Horizontal strain rate distribution on an active ice shelf rift from in-situ GPS data. *J. Global Position. Syst.*, **8**(1), 6–16

Joughin I and MacAyeal DR (2005) Calving of large tabular icebergs from ice shelf rift systems. *Geophys. Res. Lett.*, **32**(2), L02501 (doi: 10.1029/2004GL020978)

Khazendar A and Jenkins A (2003) A model of marine ice formation within Antarctic ice shelf rifts. *J. Geophys. Res.*, **108**(C7), 3235 (doi: 10.1029/2002JC001673)

Larour E, Rignot E and Aubry D (2004) Modelling of rift propagation on Ronne Ice Shelf, Antarctica, and sensitivity to climate change. *Geophys. Res. Lett.*, **31**(16), L16404 (doi: 10.1029/2004GL020077)

Leonard KC, Tremblay L-B, MacAyeal DR and Jacobs SS (2008) Interactions of wind-transported snow with a rift in the Ross Ice Shelf, Antarctica. *Geophys. Res. Lett.*, **35**(5), L05501 (doi: 10.1029/2007GL033005.)

MacAyeal DR, Okal EA, Aster RC and Bassis JN (2009) Seismic observations of glaciogenic ocean waves (micro-tsunamis) on icebergs and ice shelves. *J. Glaciol.*, **55**(190), 193–206 (doi: 10.3189/002214309788608679)

Mercer JH (1978) West Antarctic ice sheet and CO_2 greenhouse effect: a threat of disaster. *Nature*, **271**(5643), 321–325 (doi: 10.1038/271321a0)

Oza SR, Singh RKK, Vyas NK and Sarkar A (2011) Study of inter-annual variations in surface melting over Amery Ice Shelf, East Antarctica, using space-borne scatterometer data. *J. Earth Syst. Sci.*, **120**(2), 329–336 (doi: 10.1007/s12040-011-0055-8)

Pritchard HD, Ligtenberg SRM, Fricker HA, Vaughan DG, Van den Broeke MR and Padman L (2012) Antarctic ice-sheet loss driven by basal melting of ice shelves. *Nature*, **484**(7395), 502–505 (doi: 10.1038/nature10968)

Rignot E and MacAyeal DR (1998) Ice-shelf dynamics near the front of the Filchner–Ronne Ice Shelf, Antarctica, revealed by SAR interferometry. *J. Glaciol.*, **44**(147), 405–418

Rott H, Rack W, Skvarca P and De Angelis H (2002) Northern Larsen Ice Shelf, Antarctica: further retreat after collapse. *Ann. Glaciol.*, **34**, 277–282 (doi: 10.3189/172756402781817716)

Rignot E, Casassa G, Gogineni P, Krabill W, Rivera A and Thomas R (2004) Accelerated ice discharge from the Antarctic Peninsula following the collapse of Larsen B ice shelf. *Geophys. Res. Lett.*, **31**(18), L18401 (doi: 10.1029/2004GL020697)

Scambos T, Hulbe C and Fahnestock M (2003) Climate-induced ice shelf disintegration in the Antarctic Peninsula. In Domack EW, Burnett A, Leventer A, Conley P, Kirby M and Bindschadler R eds. *Antarctic Peninsula climate variability: a historical and paleoenvironmental perspective*. (Antarctic Research Series 79) American Geophysical Union, Washington, DC, 79–92

Scambos TA, Bohlander JA, Shuman CA and Skvarca P (2004) Glacier acceleration and thinning after ice shelf collapse in the Larsen B embayment, Antarctica. *Geophys. Res. Lett.*, **31**(18), L18402 (doi: 10.1029/2004GL020670)

Schulson EM (2001) Brittle failure of ice. *Eng. Fract. Mech.*, **68**(17–18), 1839–1887 (doi: 10.1016/S0013-7944(01)00037-6)

Shepherd A, Wingham D and Rignot E (2004) Warm ocean is eroding West Antarctic Ice Sheet. *Geophys. Res. Lett.*, **31**(23), L23404 (doi: 10.1029/2004GL021106)

Shepherd A, Wingham D, Wallis D, Giles K, Laxon S and Sundal AV (2010) Recent loss of floating ice and the consequent sea level contribution. *Geophys. Res. Lett.*, **37**(13), L13503 (doi: 10.1029/2010GL042496)

Vaughan DG and Doake CSM (1996) Recent atmospheric warming and retreat of ice shelves on the Antarctic Peninsula. *Nature*, **379**(6563), 328–331 (doi: 10.1038/379328a0)

Wang L, Gong P, Ying Q, Yang Z, Cheng X and Ran Q (2010) Settlement extraction in the North China Plain using Landsat and Beijing-1 multispectral data with an improved watershed segmentation algorithm. *Int. J. Remote Sens.*, **31**(6), 1411–1426 (doi: 10.1080/01431160903475332)

Weertman J (1957) Deformation of floating ice shelves. *J. Glaciol.*, **3**(21), 38–42

Wen J, Wang Y, Wang W, Jezek KC, Liu H and Allison I (2010) Basal melting and freezing under the Amery Ice Shelf, East Antarctica. *J. Glaciol.*, **56**(195), 81–90 (doi: 10.3189/002214310791190820)

Williams MJM, Warner RC and Budd WF (2002) Sensitivity of the Amery Ice Shelf, Antarctica, to changes in the climate of the Southern Ocean. *J. Climate*, **15**(19), 2740–2757 (doi: 10.1175/1520-0442(2002)015<2740:SOTAIS>2.0.CO;2)

Young NW and Hyland G (2002) Velocity and strain rates derived from InSAR analysis over the Amery Ice Shelf, East Antarctica. *Ann. Glaciol.*, **34**, 228–234 (doi: 10.3189/172756402781817842)

Yu J, Liu H, Jezek KC, Warner RC and Wen J (2010) Analysis of velocity field, mass balance, and basal melt of the Lambert Glacier–Amery Ice Shelf system by incorporating Radarsat SAR interferometry and ICESat laser altimetry measurements. *J. Geophys. Res.*, **115**(B11), B11102 (doi: 10.1029/2010JB007456)

Zhang L, Dong W, Zhang D and Shi G (2010) Two-stage image denoising by principal component analysis with local pixel grouping. *Pattern Recog.*, **43**(4), 1531–1549 (doi: 10.1016/j.patcog.2009.09.023)